JOURNAL OF SOLID STATE CHEMISTRY **131,** 394–398 (1997)
ARTICLE NO. SC977415

Chemical Bonding Topology of Superconductors

4. Heavy Fermion Superconductors

R. B. King

Department of Chemistry, University of Georgia, Athens, Georgia 30602

Received November 22, 1996; accepted April 7, 1997

Heavy fermion superconductors can be classified into the following two types based on their structures: (1) ternary transition metal carbides, borides, and silicides containing *f*-block metals exhibiting stable multiple oxidation states such as cerium in $CeCu_2Si_2$, $CeRu_3B_2$, and $CeRu_3Si_2$ or uranium in URu_2Si_2 and U_2PtC_2; (2) binary alloys containing multiple oxidation state actinides (particularly uranium) and nonactinide polyhedral clusters such as Be_{13} centered icosahedra in UBe_{13} and $Pt_{6/2}$ octahedra in UPt_3. The *f*-block metals in heavy fermion superconductors not only exhibit multiple oxidation states but are also diluted enough by the other elements so that the separation between *f*-block metals in the structure is at least 4 Å. The *f*-block metals become part of the conducting skeletons of heavy fermion superconductors so that their conductivities arise at least partially through valence fluctuations involving *f*-electrons. © 1997 Academic Press

1. INTRODUCTION

Studies reported by the author in 1987 on ternary molybdenum chalcogenides MMo_6S_8 (Chevrel phases) (2) and ternary lanthanide rhodium borides $LnRh_4B_4$ (3) using graph-theory derived methods (4, 5) have suggested a connection between relatively high superconducting critical temperatures (e.g., T_c's > 4 K) and a conducting skeleton having an edge-localized chemical bonding topology with holes in the valence band. Such ideas were subsequently extended to other types of superconductors including other ternary metal borides and silicides (6), the quaternary lanthanide nickel borocarbides and boronitrides (1), the A-15 alloy superconductors M_3E (M = V, Nb, Ta; E = Si, Ge, Sn) (6), and transition metal alloys (6). In addition, such ideas were shown to provide a simple rationalization of the unusually high T_c's of the copper oxide superconductors (7, 8).

A major category of superconductors not included in any of these studies are the so-called heavy fermion superconductors (9). The superconductivity in such heavy fermion superconductors arises from highly correlated, high-effective-mass f electrons and thus requires the presence of a lanthanide or actinide with more than one stable oxidation state to facilitate *f*-electron transfer. The first heavy fermion superconductor to be discovered was $CeCu_2Si_2$, first reported in 1979 with a T_c of 0.53 K (10). Other early examples of heavy fermion superconductors are UBe_{13} ($T_c = 0.97$ K) (11) and UPt_3 ($T_c = 0.54$ K) (12). In general, heavy fermion superconductors exhibit lower T_c's than the other types of superconductors which have been considered. Thus the highest T_c's in heavy fermion superconductors are only the ~ 1.5 K T_c's found in URu_2Si_2 (Refs. 13 and 14) U_2PtC_2 (Refs. 15 and 16).

The minimum requirements for a heavy fermion superconductor appear to be the presence of an *f*-block metal (lanthanide or actinide) exhibiting more than one stable oxidation state and a structure in which the atoms of the *f*-block metal are so diluted with other atoms so that there are no direct interactions between *f*-block metals. Within this general framework heavy fermion superconductors can be classified into two broad categories: (1) ternary heavy fermion superconductors containing the *f*-block metal, a transition or coinage metal such as a noble metal or copper, and a nonmetal or metalloid such as carbon, boron, or silicon as exemplified by $CeCu_2Si_2$, $U_2Ru_2Si_2$, and U_2PtC_2; (2) Binary heavy fermion superconductors in which the *f*-block metal (uranium in the common examples) is diluted by polyhedra of the second element such as a Pt_6 octahedron in UPt_3 or a Be_{13} centered icosahedron in UBe_{13}. This paper examines the chemical bonding topology in structures of both types.

2. BACKGROUND

Previous studies (1–3, 6, 17–22) on the chemical bonding topologies of solid state materials have first partitioned the structures into positive ions of the alkali, alkaline earth, lanthanide, or actinide metal present in the structure and a negatively charged network containing the remaining elements. In ternary and quaternary superconductors (1–3, 6), the negatively charged network has an infinite polymeric structure exhibiting edge-localized chemical bonding leading

0022-4596/97 $25.00

to porous delocalization. This negatively charged polymeric network becomes the conducting skeleton of the superconductor and typically has an electronic configuration less than the closed shell configuration leading to holes in the valence band and *p*-type conductivity. The metals forming the positive counterions in these ternary and quaternary solid state structures exhibit only a single stable oxidation state, namely +1 for the alkali metals, +2 for the alkaline earth metals, +3 for the lanthanides considered, and +4 for thorium as in Th_2NiC_2 (19, 22).

A similar method can be used to partition the structures of the heavy fermion superconductors into positive lanthanide or actinide ions and a negatively charged polymeric skeleton containing the other elements. The major difference arises from the multiple oxidation states of the lanthanide or actinide positive ions so that these cations as well as the negatively charged polymeric network can participate in the electron transport required for superconductivity. Thus the entire structure of a heavy fermion superconductor rather than only the anionic network becomes the conducting skeleton. Since the variable oxidation states of the lanthanide or actinide cations result from different numbers of *f* electrons, participation of the cations as well as the anionic network in electron transport necessarily involves the *f* electrons of the cations leading to heavy fermion behavior. Such heavy fermion behavior not only includes superconductivity but also magnetic ordering with anomalously high ordering temperature, the Kondo effect, and other types of mixed valence (23) behavior (24). The sets of *f*-block metal oxidation states involved in heavy fermion superconductors include particularly Ce(III)↔Ce(IV) and U(III)↔U(IV)↔U(V)↔U(VI), although Yb(II)↔Yb(III) and Np(III)↔Np(IV)↔Np(V)↔Np(VI) oxidation state sets are involved in other heavy fermion materials (9). In the ternary heavy fermion structures analogous compounds are almost always known containing *f*-block elements exhibiting single oxidation states and *f*-block elements exhibiting multiple oxidation states. The chemical bonding topology and electron count of the structures with the single oxidation state *f*-block elements can thus first be examined for comparison with the analogous structures containing multiple oxidation state *f*-block elements. In many cases the chemical bonding topology of the single oxidation state countercation analogue has already been examined in an earlier paper (6). The ternary heavy fermion superconductor structures of interest are listed in Table 1.

3. TERNARY HEAVY FERMION SUPERCONDUCTORS

3.1. $BaAl_4$ Type Structures

The chemical bonding topology of superconducting metal silicides with the $BaAl_4$ structure was examined in an earlier paper (6). The aluminum network in the $BaAl_4$ structure (Fig. 1) consists of basal edge-sharing $Al^aAl^b_{4/4}$ square pyramids of aluminum atoms similar to the isolated B_5H_9 square pyramid. The stability of $BaAl_4$ suggests the stability of a polymeric Al_4^{2-} anion containing 14 valence electrons per formula unit. In the heavy fermion superconductor $CeCu_2Si_2$ with a closely related structure (25) the *neutral* Cu_2Si_2 subnetwork has a total of 10 valence electrons assuming one valence electron for each copper atom (i.e., Cu(I) with a filled d^{10} shell) and four valence electrons each for each silicon atom. Thus $Cu_2Si_2^{4-}$ with a Ce^{4+} counterion and Cu(I) in $CeCu_2Si_2$ is isoelectronic with Al_4^{2-} in $BaAl_4$ with a Ba^{2+} counterion, since each has 14 valence electrons. Electronic conduction in $CeCu_2Si_2$ can occur through the synchronized valence changes Ce(III)↔Ce(IV) and Cu(I)↔Cu(II) based on the stable oxidation states of cerium and copper. Thus the 14 valence electrons per $CeCu_2Si_2$ unit can arise from Ce(IV) + 2Cu(I) or Ce(III) + Cu(II) + Cu(I). In the related compounds $EuCu_2Si_2$ and $YbCu_2Si_2$, not known to be superconductors the lanthanide counterions have the oxidation state pairs Ln(II)↔Ln(III) rather than Ln(III)↔Ln(IV), so the favored 14 valence electrons must arise from Ln(III) + Cu(II) + Cu(I) or Ln(II) + 2Cu(II). This difference between $EuCu_2Si_2$ and $YbCu_2Si_2$, on the one hand, and $CeCu_2Si_2$, on the other hand, is expected to lead to significant differences in electronic behavior between these two types of materials in accord with experimental observations.

The other heavy fermion superconductor with the $BaAl_4$ structure is URu_2Si_2 ($T_c = 1.5$ K) (13, 14), which may be related to $LaIr_2Si_2$, which is also a superconductor (26) with $T_c = 1.6$ K. The $Ir_2Si_2^{3-}$ anion in $LaIr_2Si_2$ has 29 valence electrons (including the Ir *d* electrons) and is thus isoelectronic with a 29-valence electron $Ru_2Si_2^{5-}$, implying an average +5 oxidation state for the uranium countercation to attain electroneutrality. This is consistent with uranium

TABLE 1
Types of Ternary Heavy Fermion Superconductor Structures

Single oxidation state countercations	Multiple oxidation state countercations	Known heavy fermion superconductors
$LaIr_2Si_2$ ($BaAl_4$ structure)	$EuCu_2Si_2$, $YbCu_2Si_2$	$CeCu_2Si_2$, URu_2Si_2
$LuOs_3B_2$	$CeIr_3Si_2$, $CeIr_3B_2$	$CeRu_3B_2$, $CeOs_3B_2$, $CeRu_3Si_2$
LaPtSi, ThIrSi	CeNiSn, CeNiIn, CeRhIn, CeIrGe, CeRhSb, YbCuGa	
Th_2NiC_2	U_2RuC_2, U_2OsC_2, U_2IrC_2, U_2RhC_2	U_2PtC_2

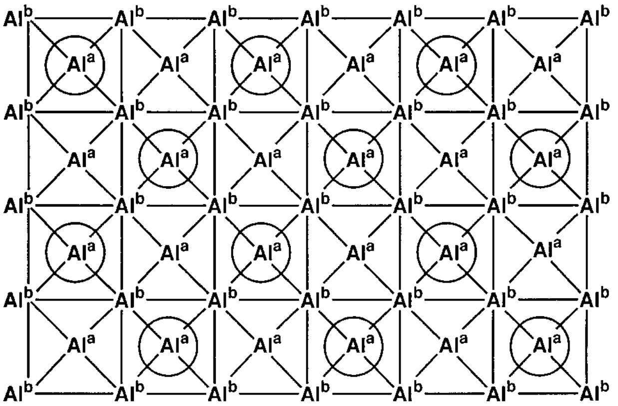

FIG. 1. A schematic view of a portion of the aluminum network in $BaAl_4$. Circled aluminum atoms inside the squares appear in front of the page whereas uncircled aluminum atoms appear in back of the pages. Each $Al^aAl^b_{4/4}$ square corresponds to a square pyramidal cavity.

valence fluctuations in the $U(IV) \leftrightarrow U(V) \leftrightarrow U(VI)$ range leading to heavy fermion behavior for URu_2Si_2.

3.2. $LuOs_3B_2$ *Type Structures*

The $LuOs_3B_2$ type structure, which was discussed in the earlier paper (6), contains boron-centered transition metal trigonal prisms (27). Each transition metal atom is shared by four such trigonal prisms so that the fundamental structural unit of the anionic network in $LuOs_3B_2$ is the trigonal prismatic cavity $Os_{6/4}B$. The bonding topology within such a centered trigonal prismatic cavity is expected to be edge-localized similarly to that in the discrete centered trigonal prismatic $[Co_6(CO)_{15}C]^{2-}$ anion (28, 29). In $LuOs_3B_2$ each of the nine edges of a single $Os_{6/4}B$ trigonal prism is shared between two such trigonal prisms so that a closed-shell electronic configuration for edge-localized bonding has $(2)(9/2) = 9$ skeletal electrons per trigonal prism, corresponding to $Os_{6/4}B^{3-} = Os_3B_2^{6-}$, with each osmium vertex using six internal orbitals and thus serving as a donor of two skeletal electrons (6). Thus in $LuOs_3B_2$ each $Os_{6/4}B^{1.5-}$ boron-centered trigonal prism lacks 1 1/2 electrons of the closed-shell electronic configuration leading to holes in its valence band. In $CeRu_3B_2$ and $CeOs_3B_2$ oxidation of Ce(III) to Ce(IV) increases the negative charge from $M_{6/4}B^{1.5-}$ to $M_{6/4}B^{2-}$ thereby partially filling the holes in the valence band of the anionic network. The corresponding silicides such as $CeRu_3Si_2$ have an analogous structure with a silicon-centered trigonal prism so that $Ru_{6/4}Si^{2-}$, isoelectronic with $Os_{6/4}B^{3-}$, is the closed-shell electronic configuration. If the cerium counterion is Ce(IV), then the anionic network in $CeRu_3Si_2$ has this closed shell electronic configuration with a filled valence band. Electron transport in $CeRu_3Si_2$ can occur through reduction of Ce(IV) to Ce(III) concurrently removing an electron from its filled valence band. The physical properties of the known $CeIr_3Si_2$ with an analogous structure correspond to cerium in the purely trivalent state. In this case $Ir_{6/4}Si^{0.5-}$ is the closed shell electronic configuration so that $CeIr_3Si_2$ with trivalent cerium (the lowest stable oxidation state of cerium) is a *n*-type material with electrons in the conduction band. Thus the series of isostructural materials $LuOs_3B_2 \rightarrow CeIr_3B_2 \rightarrow CeIr_3Si_2$ represent a transition from *p*-type conductors with holes in the valence band to *n*-type conductors with electrons in the conduction band.

3.3. *LaPtSi Structures*

The isostructural and isoelectronic superconductors LaPtSi ($T_c = 3.5$ K) (30) and ThIrSi ($T_c = 6.5$ K) (31) have structures containing neither transition metal–metal nor silicon–silicon homonuclear bonds (6). Each transition metal is bonded to three silicon atoms and each silicon atom is bonded to three transition-metal atoms, leading to the building blocks $PtSi_{3/3}^{3-}$ and $IrSi_{3/3}^{4-}$ for the anionic networks in LaPtSi and ThIrSi, respectively. In these building blocks each transition metal has 17 average valence electrons, which is one electron less than the favored 18-electron closed-shell noble gas configuration, thereby leading to holes in the valence band. A variety of isostructural species are known that contain variable oxidation state lanthanides (Table 2) in which the electronic configuration of the central transition metal is related to the oxidation state of the lanthanide countercation.

3.4. Th_2NiC_2 *Structures*

The structure of Th_2NiC_2 contains isolated linear $[C{-}Ni{-}C]^{8-}$ anions with 26 valence electrons and Ni–C distances of 1.93 Å, suggestive of Ni–C single bonding (32). Assignment of the usual $+4$ and -4 oxidation states to the Th and isolated carbon atoms, respectively, leads to a formal oxidation state of zero for the nickel atom. The NiC_2^{8-}

TABLE 2
Electronic Configurations of Materials with the LaPtSi Structure

Transition Metal Valence Electrons				
15	16	17	18	References
		$La^{III}PtSi$		(30)
		$Ce^{III}NiSn$	$Ce^{IV}NiSn$	
	$Ce^{III}NiIn$	$Ce^{IV}NiIn$		
		$Th^{IV}IrSi$		(31)
		$Ce^{III}RhSb$	$Ce^{IV}RhSb$	
	$Ce^{III}IrGe$	$Ce^{IV}IrGe$		
$Ce^{III}RhIn$	$Ce^{IV}RhIn$			
	$Yb^{II}CuGa$	$Yb^{III}CuGa$		

anion is thus an example of a linear d^{10} metal derivative in which the nickel atom has the favored 14-electron configuration for a two-coordinate linear derivative using a seven-orbital spd^5 bonding manifold (33).

The Th_2NiC_2 structure is found in a variety of uranium transition metal carbides U_2MC_2 (M = Ru, Os, Rh, Ir, Pt) (34). The platinum compound U_2PtC_2 exhibits heavy fermion superconductivity ($T_c = 1.5$ K) and a magnetic susceptibility corresponding to two unpaired electrons per formula unit, suggesting U(IV) and the formulation $U^{IV}_2PtC_2$ containing the closed shell PtC_2^{8-} anion, isoelectronic with the NiC_2^{8-} anion in Th_2NiC_2. The strong paramagnetism of U_2RuC_2 and U_2OsC_2, which exhibits a weak temperature dependence, suggests an intermediate uranium oxidation state and linear diamagnetic RuC_2^{10-} and OsC_2^{10-} anions with a 14-electron configuration similar to that in the isoelectronic NiC_2^{8-} in Th_2NiC_2 discussed above (34). If U_2RuC_2 and U_2OsC_2 are formulated with the anions RuC_2^{10-} and OsC_2^{10-}, respectively, then the average uranium oxidation state becomes +5. However, the temperature-dependent paramagnetism of U_2RhC_2 and U_2IrC_2 suggests RhC_2^{8-} and IrC_2^{8-} anions with one unpaired electron per transition metal site (34).

4. OTHER HEAVY FERMION SUPERCONDUCTORS

4.1. *UBe*$_{13}$

The beryllium network in UBe_{13} consists of $Be^{(1)}Be^{(2)}_{12}$ centered icosahedra packed to form larger 24-atom irregular snub cube cavities of $Be^{(2)}$ atoms surrounding the uranium atoms (Fig. 2) (35). The shortest U ··· U distances are 5.13 Å, thereby precluding any direct uranium–uranium interaction. Each $Be^{(2)}$ vertex atom of the Be_{12} icosahedra is bonded to four external beryllium vertices of adjacent icosahedra. Since each such beryllium vertex atom has only one external orbital, these external bonds necessarily must be five-center $Be^{(2)}_5$ bonds for which each of the five beryllium atoms donates an average of 2/5 electron to provide an electron pair for the bonding orbital of its five-center external bond. A neutral beryllium atom has two valence electrons, so that a *neutral* $Be^{(1)}Be^{(2)}_{12}$ centered icosahedron has exactly the 26 skeletal electrons corresponding to the $2n + 2$ for $n = 12$ for globally delocalized bonding analogous to that in the very stable icosahedral anion $B_{12}H_{12}^{2-}$ if *no* electrons are left for the external bonds to the adjacent $Be^{(1)}Be^{(2)}_{12}$ centered icosahedra. Since these external bonds are five-center $Be^{(2)}_5$ bonds, there are an average of 12/5 such bonds requiring $24/5 = 4.8$ valence electrons for each $Be^{(1)}Be^{(2)}_{12}$ centered icosahedron corresponding to $Be_{13}^{-4.8}$ for a closed-shell electronic configuration leading to an average uranium oxidation state of +4.8. This is well within the stable uranium oxidation state manifold U(IV) ↔ U(V) ↔ U(VI) so that average uranium oxidation states below +4.8 correspond to holes in the valence band of the beryllium network and average uranium oxidation states above +4.8 correspond to electrons in the conduction band of the beryllium network. Thus in UBe_{13} the uranium valence fluctuations can lead to heavy fermion behavior including heavy fermion superconductivity.

4.2. *UPt*$_3$

The structure of UPt_3 consists of a lattice of face-centered $U_{8/8}Pt_{6/2}$ cubes (Fig. 3) with the uranium atoms at the vertices and the platinum atoms in the centers of the faces (36). Each uranium atom is thus shared by eight such cubes, whereas each platinum atom is shared by the two cubes sharing the face containing the platinum atom. The $U_{88}Pt_{6/2}$ building blocks thus correspond to $Pt_{6/2}$ octahedra within uranium cubes. The network of vertex-sharing $Pt_{6/2}$ octahedra separates the uranium atoms in the UPt_3 structure so that the minimum U ··· U distance is 4.1 Å. Consider these $Pt_{6/2}$ octahedra to be globally delocalized octahedra requiring three internal orbitals from

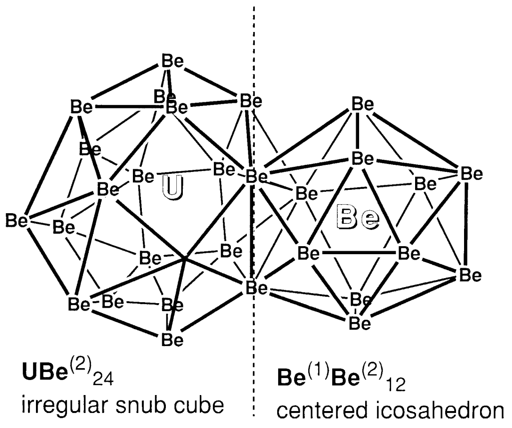

FIG. 2. The $Be^{(1)}Be^{(2)}_{12}$ icosahedron and $UBe^{(1)}_{24}$ irregular snub cube building blocks of the UBe_{13} structure, showing their linkage.

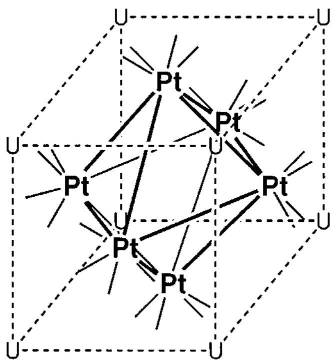

FIG. 3. The $U_{8/8}Pt_{6/2}$ building block of the UPt_3 structure, showing the $Pt_{6/2}$ octahedron within the $U_{8/8}$ cube.

each vertex atom. Each platinum atom thus uses six of the nine orbitals of its sp^3d^5 manifold for skeletal bonding to the two octahedra of which it is a part leaving three external orbitals. Filling these three external orbitals of each platinum atom with nonbonding electron pairs requires 6 of its 10 valence electrons, leaving 4 valence electrons per platinum atom for skeletal bonding. Since a globally delocalized $\mathrm{Pt}_{6/2}$ octahedron requires 14 ($= 2n + 2$ for $n = 6$) skeletal electrons, the closed shell configuration for the platinum subnetwork is obtained for $\mathrm{Pt}_{6/2}^{2-}$. Since the lowest likely oxidation state for uranium in UPt_3 is $+4$, corresponding to a $\mathrm{Pt}_{6/2}^{4-}$ closed shell electronic configuration, the compound UPt_3 is electron-rich with electrons in its conduction band. The fact that UPt_3 is electron richer than any other of the heavy fermion superconductors may account for some of its unusual properties compared with other heavy fermion superconductors (37).

5. CONCLUSIONS

This work suggests that heavy fermion superconductors can be classified into the following two types based on their structures:

(1) Ternary transition metal carbides, borides, or silicides containing *f*-block metals exhibiting multiple stable oxidation states such as uranium or cerium;

(2) Binary alloys of multiple oxidation state actinides containing distinct non-actinide polyhedral clusters such as Be_{13} centered icosahedra in UBe_{13} and $\mathrm{Pt}_{6/2}$ octahedra in UPt_3.

The *f*-block metals in heavy fermion superconductors not only exhibit multiple oxidation states but are also diluted enough by the other elements so that the separation between *f*-block metals in the structure is at least 4 Å. The *f*-block metals become part of the conducting skeletons of heavy fermion superconductors so that their conductivities arise at least partially through *f*-block metal valence fluctuations involving their *f*-electrons.

REFERENCES

1. For part 3 of this series see R. B. King, *J. Solid State Chem.* **124,** 329 (1996).
2. R. B. King, *J. Solid State Chem.* **71,** 224 (1987).
3. R. B. King, *J. Solid State Chem.* **71,** 233 (1987).
4. R. B. King and D. H. Rouvray, *J. Am. Chem. Soc.* **99,** 7834 (1977).
5. R. B. King, "Applications of Graph Theory and Topology in Inorganic Cluster and Coordination Chemistry," CRC Press, Boca Raton, FL, 1993.
6. R. B. King, *Inorg. Chem.* **29,** 2164 (1990).
7. R. B. King, *Inorg. Chim. Acta* **15,** 143 (1988).
8. R. B. King, *J. Mater. Sci. Lett.* **9,** 5 (1990).
9. G. R. Stewart, *Rev. Mod. Phys.* **59,** 755 (1984).
10. F. Steglich, J. Aarts, C. D. Bredl, W. Lieke, D. Meschede, W. Franz, and J. Schäfer, *Phys. Rev. Lett.* **43,** 1892 (1979).
11. H. R. Ott, H. Rudigier, Z. Fisk, and J. L. Smith, *Phys. Rev. Lett.* **50,** 1595 (1983).
12. G. R. Stewart, Z. Fisk, J. O. Willis, and J. L. Smith, *Phys. Rev. Lett.* **52,** 679 (1984).
13. Y. Dalichaouch, M. B. Maple, J. W. Chen, T. Kohara, C. Rossel, M. S. Torikachvili, and A. L. Giorgi, *Phys. Rev.* **41,** 1829 (1990).
14. C. Boholm, J. K. Kjems, W. J. L. Buyers, P. Matthew, T. T. M. Palstra, A. A. Menovsky, and J. A. Mydosh, *Phys. Rev. Lett* **58,** 1467 (1987).
15. G. P. Meisner, A. L. Giorgi, A. C. Lawson, G. R. Stewart, J. O. Willis, M. S. Wire, and J. L. Smith, *Phys. Rev. Lett.* **53,** 1829 (1984).
16. F. Marabelli and P. Wachter, *Solid State Comm.* **74,** 1075 (1990).
17. R. B. King, *Polyhedron* **7,** 1813 (1988).
18. R. B. King, *Inorg. Chem.* **28,** 2796 (1989).
19. R. B. King, *Russ. Chem. Bull.* **43,** 1533 (1994).
20. R. B. King, *Inorg. Chim. Acta* **228,** 219 (1995).
21. R. B. King, *Canad. J. Chem.* **73,** 963 (1995).
22. R. B. King, *J. Organometal. Chem.*, in press.
23. M. B. Robin and P. Day, *Adv. Inorg. Chem. Radiochem.* **10,** 247 (1967).
24. D. T. Androja and S. K. Malik, *J. Magn. Magn. Mater.* **100,** 126 (1991).
25. D. Rossi, R. Marazza, and R. Ferro, *J. Less-Common Met.* **66,** 17 (1979).
26. H. F. Braun, *J. Less-Common Met.* **100,** 105 (1984).
27. K. Niihara and S. Yajima, *Bull. Chem. Soc. Jpn.* **46.** 770 (1973).
28. S. Martinengo, D. Strumolo, P. Chinik, V. G. Albano, and D. Braga, *J. Chem. Soc. Dalton Trans.*, 35 (1985).
29. R. B. King, *New J. Chem.* **12,** 493 (1988).
30. J. Evers, G. Oehlinger, A. Weiss, and C. Probst, *Solid State Commun.* **50,** 61 (1984).
31. P. Lejay, B. Chevalier, J. Etourneau, M. J. Tarascon, and P. Hagenmuller, *Mater. Res. Bull.* **18,** 67 (1983).
32. M. A. Moss and W. Jeitschko, *Z. Anorg. Allgem. Chem.* **603,** 57 (1991).
33. R. B. King, *J. Chem. Inf. Comp. Sci.* **34,** 410 (1994).
34. T. Ebel, K.-H. Wachtmann, and W. Jeitschko, *Solid State Commun.* **97,** 815 (1996).
35. M. W. McElfrish, J. H. Hall, R. R. Ryan, J. L. Smith, and Z. Fisk, *Acta Crystallogr. Sect. C* **46,** 1579 (1990).
36. T. J. Heal and G. I. Williams, *Acta Crystallogr.* **8,** 494 (1955).
37. G. R. Stewart, *J. Appl. Phys.* **57,** 3049 (1985).